NuSAP, a Mitotic RanGTP Target That Stabilizes and Cross-links Microtubules □D

**Katharina Ribbeck,* Aaron C. Groen,†‡ Rachel Santarella,*‡
Markus T. Bohnsack,‡§ Tim Raemaekers,‡∥ Thomas Köcher,¶ Marc Gentzel,*
Dirk Görlich,§ Matthias Wilm,* Geert Carmeliet,# Timothy J. Mitchison,†
Jan Ellenberg,* Andreas Hoenger,@ and Iain W. Mattaj***

*European Molecular Biology Laboratory, D-69117 Heidelberg, Germany; †Department of Systems Biology, Harvard Medical School, Boston, MA 02115; §Zentrum für Molekulare Biologie Heidelberg, D-69120 Heidelberg, Germany; ∥Membrane Trafficking Laboratory, Center for Human Genetics/VIB04, Katholieke Universiteit Leuven, B-3000 Leuven, Belgium; ¶Uppsala Biomedical Centrum, SE-75 123 Uppsala, Sweden; #Laboratory for Experimental Medicine and Endocrinology, Katholieke Universiteit Leuven, Gasthuisberg, B-3000 Leuven, Belgium; and @The Boulder Laboratory for 3-D Electron Microscopy of Cells, University of Colorado, Boulder, CO 80309

Nucleolar and spindle-associated protein (NuSAP) was recently identified as a microtubule- and chromatin-binding protein in vertebrates that is nuclear during interphase. Small interfering RNA-mediated depletion of NuSAP resulted in aberrant spindle formation, missegregation of chromosomes, and ultimately blocked cell proliferation. We show here that NuSAP is enriched on chromatin-proximal microtubules at meiotic spindles in *Xenopus* oocytes. When added at higher than physiological levels to *Xenopus* egg extract, NuSAP induces extensive bundling of spindle microtubules and causes bundled microtubules within spindle-like structures to become longer. In vitro reconstitution experiments reveal two direct effects of NuSAP on microtubules: first, it can efficiently stabilize microtubules against depolymerization, and second, it can cross-link large numbers of microtubules into aster-like structures, thick fibers, and networks. With defined components we show that the activity of NuSAP is differentially regulated by Importin (Imp) α, Impβ, and Imp7. While Impα and Imp7 appear to block the microtubule-stabilizing activity of NuSAP, Impβ specifically suppresses aspects of the cross-linking activity of NuSAP. We propose that to achieve full NuSAP functionality at the spindle, all three importins must be dissociated by RanGTP. Once activated, NuSAP may aid to maintain spindle integrity by stabilizing and cross-linking microtubules around chromatin.

INTRODUCTION

The small GTPase Ran controls several key cellular processes. It provides the energy required for nuclear transport and guides spindle assembly at the onset of mitosis and nuclear envelope reassembly at the end of mitosis (Görlich, 1998; Hetzer *et al.*, 2000; Zheng, 2004). Like all GTPases, Ran binds to GTP and catalyzes its hydrolysis to GDP. The GTPase activating protein (RanGAP), in a complex with RanBP1/2, stimulates the intrinsically low GTPase activity of Ran and thereby depletes RanGTP from the cytoplasm. Chromosome-associated RCC1 directly antagonizes the activity of RanGAP by accelerating the nucleotide exchange of GDP for GTP, generating RanGTP around chromatin (Ohtsubo *et al.*, 1989).

Transport receptors of the Importin (Imp) β family (TRs) are the immediate effectors of RanGTP. Cargo-molecules associate with TRs in a Ran-regulated manner. They can thus be considered as the downstream targets of RanGTP. The human genome encodes 20 members of the Impβ family (Görlich *et al.*, 1997), which are typically classified as importins and exportins. Importins bind their cargo at low RanGTP levels (Rexach and Blobel, 1995; Görlich *et al.*, 1996; Chi *et al.*, 1997; Izaurralde *et al.*, 1997; Siomi *et al.*, 1997; Jäkel and Görlich, 1998) and release it on direct binding of RanGTP to the importin. Exportins operate in the opposite manner; they bind their substrates efficiently only in the presence of RanGTP (Fornerod *et al.*, 1997; Kutay *et al.*, 1997) and dissociate from the cargo upon GTP hydrolysis by Ran.

A key recent finding to understanding Ran function was that TRs not only direct the localization of a cargo but also influence cargo activity (Karsenti and Vernos, 2001; Hetzer *et al.*, 2002; Zheng, 2004). One example is in spindle organization. It has been shown that certain spindle-assembly factors are inactivated by importin binding and that they are activated by RanGTP-dependent importin release (Hetzer *et al.*, 2002; Zheng, 2004). The presence of RCC1 on chromatin stimulates the production of RanGTP and thus activates mitotic regulators and triggers spindle assembly around

chromatin (Carazo-Salas *et al.*, 1999; Kalab *et al.*, 1999; Ohba *et al.*, 1999; Wilde and Zheng, 1999).

The organization of the spindle requires that the activity of many, probably hundreds of proteins is tightly regulated in both time and space. Ran is one key coordinator of these activities. An integrated view of spindle assembly thus not only requires knowledge of specific spindle factor activities but also of how these activities are coupled to the RanGTP network.

NuSAP was discovered as an essential microtubule-binding protein in proliferating cells (Raemaekers *et al.*, 2003). Two key features suggested that NuSAP might be a component of the mitotic RanGTP network: 1) NuSAP is actively imported into the nucleus during interphase, and 2) NuSAP localizes to the spindle during mitosis. This prompted us to study NuSAP activity and Ran-dependent regulation in detail.

We here identify NuSAP as a mitotic RanGTP target. When added at higher than physiological levels to *Xenopus* egg extract, NuSAP increases the microtubule-bundling capacity of the extract and the length of in vitro assembled spindle-like structures. This observation can be explained by the effects of recombinant NuSAP on microtubules in vitro. Reconstitution experiments with defined components show that NuSAP can efficiently prevent microtubules from depolymerization, and, in addition, cross-link them into networks and bundles. We further show that Impα, Impβ, and Imp7 are direct regulators of NuSAP activity. Importantly, each importin affects a different aspect of NuSAP function. Whereas Impα and Imp7 appear to block the microtubule-stabilizing activity of NuSAP, Impβ suppresses specifically its cross-linking activity. We propose a model where, at chromatin, RanGTP needs to dissociate all three importins from NuSAP to achieve full functionality of the protein.

MATERIALS AND METHODS

Identification of X. laevis NuSAP

Multiple expressed sequence tags from *X. laevis* and *X. tropicalis* were identified and assembled from the National Center for Biotechnology Information database based on their homology to human or mouse NuSAP to yield the full-length *X. laevis* NuSAP open reading frame (accession DQ448820).

Expression, Purification, and Fluorescence Labeling of Recombinant Proteins

RanQ69L, Impα (Rch1), Impβ, and Imp7 were produced as described previously (Mingot *et al.*, 2001). Full-length *Xenopus* NuSAP was expressed from a pQE80 derivative as an N-terminally deca-histidine–tagged protein. The zz-tagged NuSAP was expressed from zzTev80N with an N-terminal double protein A tag and a C-terminal deca-histidine tag. Both NuSAP proteins were purified by nickel-NTA affinity chromatography and subsequent gel filtration for buffer exchange to 20 mM HEPES, pH 7.5, 500 mM NaCl, 5 mM magnesium acetate, 250 mM sucrose, and 1 mM dithiothreitol (DTT).

For the labeling reaction, NuSAP was incubated with a stoichiometric amount of Alexa 488 C_5 maleimide (Invitrogen, Carlsbad, CA) in 20 mM HEPES, pH 7.5, 500 mM NaCl on ice for 1 h. Unbound dye was removed by gel filtration.

Immunofluorescence in X. laevis Oocytes

Anti-NuSAP antibodies were raised in rabbits against the full-length recombinant protein and affinity purified with the antigen. Maturation and fixation of oocytes and immunofluorescence were performed essentially as described previously (Schwab *et al.*, 2001). Maturation was induced by treatment of oocytes with 5 μg/ml progesterone. NuSAP was detected with an affinity-purified anti-*Xenopus* NuSAP antibody from rabbit, and tubulin was detected with an anti-α-tubulin antibody from mouse (T9026; Sigma-Aldrich, St. Louis, MO). Rabbit and mouse primary antibodies were visualized with secondary antibodies coupled to Alexa 568 and Alexa 647 (Invitrogen), respectively. DNA was stained with Sytox Green (Molecular Probes).

In Vitro Microtubule Stabilization Assay

Rhodamine tubulin was produced as described previously (Hyman *et al.*, 1991). For the microscopic analysis, unlabeled tubulin was spiked with rhoda-

mine tubulin and polymerized at a concentration of 50 μM in BrB80 (Brinkley, 1985) with 1 mM GTP at 37°C for 10 min. The polymerized microtubules were then diluted 1:10 into a reaction buffer consisting of 20 mM HEPES, pH 7.5, 150 mM NaCl, 2 mM $MgCl_2$, 50 mg/ml Ficoll and dextran as crowding reagents, and, where indicated, 0.7 μM of recombinant NuSAP. The reaction volume was 25 μl. To test the effect of importins in this reaction, 5 μM of the TRs were preincubated with 0.7 μM NuSAP for 5 min on ice before the microtubules were added. The reaction proceeded for 10 min at room temperature (RT). In Figure 5B, GTP was omitted in the dilution buffer, and the reaction occurred for 30 s. The reaction with Alexa 488-labeled NuSAP (Figure 6) was monitored in the absence of fixatives.

To separate soluble from polymerized tubulin in microtubule pelleting assays, the reaction was scaled up to 40 μl and after 10-min incubation at RT, it was spun at $35,000 \times g$ for 10 min. Pellet and supernatant were suspended in sample buffer and subjected to SDS-PAGE and Coomassie staining. Half of the pellet and a quarter of the supernatant fraction were applied on the gel.

Electron Microscopy

Purified tubulin (20 μM) was incubated either alone or with recombinant NuSAP (2 μM) in BrB80 buffer containing 2 mM GTP. The reaction was carried out for 10 min at 37°C. Reactions were spotted on holey-carbon film, washed with water, and quick-frozen into liquid ethane as described previously by Dubochet *et al.* (1988). Images were taken on a CM-200 FEG electron microscope and an FEI Morgagni microscope.

Spindle Assembly Reactions in Extract

A rough estimate of endogenous NuSAP concentration in extract is 20–50 nM. This value was obtained by comparing NuSAP protein in extract to defined amounts of recombinant protein. For depletion, α-NuSAP antibody or IgG was immobilized on Protein A beads (Dynal Biotech, Oslo, Norway). Then, 150 μl of saturated beads was incubated with 100 μl of cytostatic factor (CSF) extract at 4°C in three consecutive rounds for 1 h each. Spindles were assembled with DNA beads, which were converted into chromatin in the depleted extracts (Lohka and Masui, 1984; Heald *et al.*, 1996; Desai *et al.*, 1999).

Protein Binding Assays

Meiotic *Xenopus* egg extract (Desai *et al.*, 1999) was spun at $350,000 \times g$ for 10 min at 4°C, and the clear supernatant was used for the binding assay. The zz-tagged NuSAP was immobilized to IgG-Sepharose beads (Pharmacia, Freiburg, Germany). Then, 20 μl of the saturated beads was incubated with 200 μl of the "high-speed" egg extract, which contained an energy regenerating system, and, where indicated, 20 μM RanQ69L. The samples were rotated for 4 h at 4°C and then washed with 20 mM HEPES-KOH (pH 7.5), 200 mM NaCl, and 5 mM $MgCl_2$. NuSAP interacting proteins were eluted with 1 M $MgCl_2$, precipitated with 95% isopropanol, and subsequently analyzed by sodium dodecyl sulfate-polyacrylamide gel electrophoresis (SDS-PAGE) and Coomassie staining. For binding assays with the recombinant proteins, NuSAP-IgG beads were incubated with 50 mM Tris-HCl, pH 7.5, 200 mM NaCl, and 5 mM magnesium acetate. Recombinant TRs and RanQ69L were added at final concentration of 2 and 35 μM, respectively, and in combinations as indicated in the figure legends.

Nuclear Import Assay

Permeabilized HeLa cells were prepared as described previously (Adam *et al.*, 1990; Ribbeck and Görlich, 2001). The import reactions were performed in transport buffer consisting of 20 mM HEPES-KOH, pH 7.5, 110 mM potassium acetate, 5 mM magnesium acetate, 250 mM sucrose, and 0.5 mM EGTA. The import reactions contained 0.5 μM fluorescent NuSAP, 1.5 μM of the individual import receptors, the components of the Ran system (3 μM Ran, 0.6 μM NTF2, 0.2 μM RanBP1, and 0.1 μM Rna1p), and an energy regenerating system (10 mM creatine phosphate, 50 μg/ml creatine kinase, 0.5 mM GTP, and 0.5 mM ATP). The reaction was carried out at RT for 20 min and then monitored by live confocal microscopy.

Mass Spectrometry

Acetonitrile, high-performance liquid chromatography grade water, DTT, iodoacetamide, formic acid (all purchased from Merck, Darmstadt, Germany), and ammonium bicarbonate (Sigma-Aldrich) were of analytical grade or better. Coomassie-stained SDS-gel bands were excised from the gel and protein in-gel digestion was performed with modified sequencing grade trypsin (Roche Diagnostics, Mannheim, Germany) as described previously (Shevchenko *et al.*, 1996), but with 10 mM ammonium bicarbonate buffer during digestion. Matrix-assisted laser desorption ionization (MALDI) mass spectrometric spectra were acquired with a MALDI time of flight (TOF)/TOF Ultraflex instrument with PAN-Upgrade installed (Bruker Daltonik, Bremen, Germany). Samples were prepared on AnchorChip 600/384 targets with α-cyano-4-hydroxy-cinnamic acid according to the dried droplet method with on-target recrystallization (Bruker Daltonik). Data interpretation was performed in-house with the MASCOT, version 2.0 search engine for mass spectrometric data (Matrixscience, London, United Kingdom; http://www.matrixscience.com).
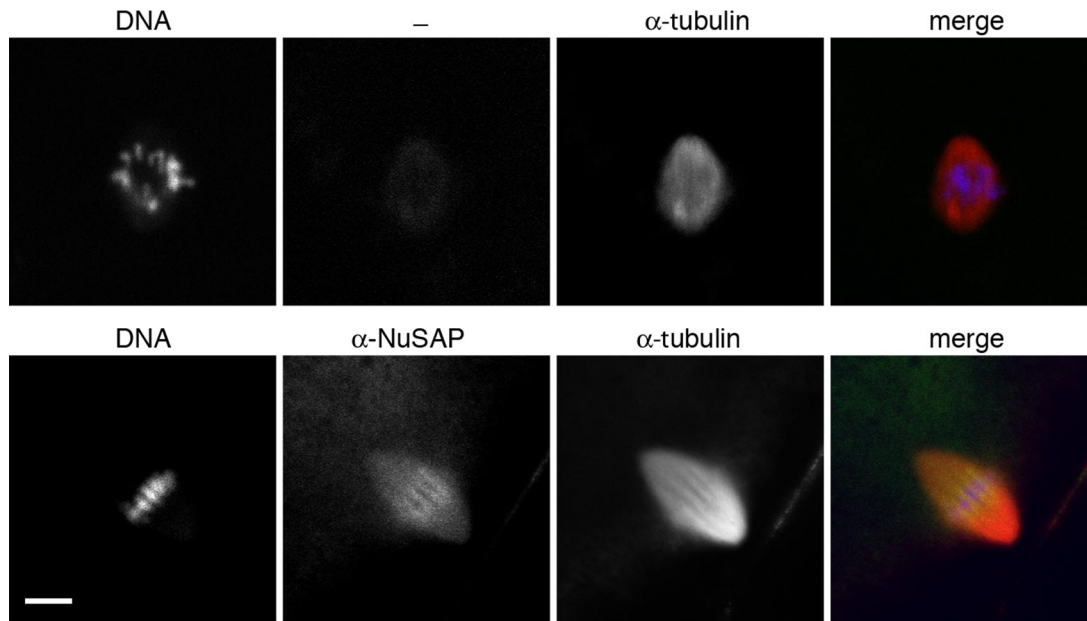
Figure 1. NuSAP localizes to microtubules and is enriched around chromatin of the meiotic spindle of *Xenopus* oocytes. Stage 6 oocytes were treated with 5 µg/ml progesterone to induce maturation. The oocytes were fixed and stained with a rabbit anti-*Xenopus* NuSAP, a mouse anti-α-tubulin antibody, and the corresponding fluorescent secondary antibodies. As a control for the NuSAP staining, the α-NuSAP antibody was omitted (top). NuSAP staining is in green, α-tubulin is in red, and DNA is in blue. Bar, 10 µm.

RESULTS

NuSAP Is Enriched at Meiotic Spindles in Xenopus Oocytes

NuSAP was discovered as a microtubule-interacting protein that is conserved in vertebrates and essential for progression through mitosis in cultured mammalian HeLa cells (Raemaekers *et al.*, 2003). It was shown that NuSAP localizes specifically to spindle microtubules that are in proximity to chromatin throughout metaphase and anaphase. This particular distribution has not been observed for other microtubule-binding proteins, and it prompted us to study NuSAP and its mechanism of function in detail. As a first step, we asked whether NuSAP is also detectable on meiotic spindles using *Xenopus* oocytes as an example. We cloned and expressed full-length NuSAP from *Xenopus*, generated antibodies, and analyzed the distribution of NuSAP on meiotic spindles in intact *X. laevis* oocytes by indirect immunofluorescence (Figure 1). Indeed, the NuSAP protein was detectable on the entire length of the metaphase spindle microtubules. As in HeLa cells, the NuSAP protein was enriched at microtubules in the immediate vicinity of chromatin in the oocytes (Figure 1). The localization of NuSAP was similar in spindles assembled with DNA beads and sperm chromatin in meiotic *Xenopus* egg extracts (our unpublished data).

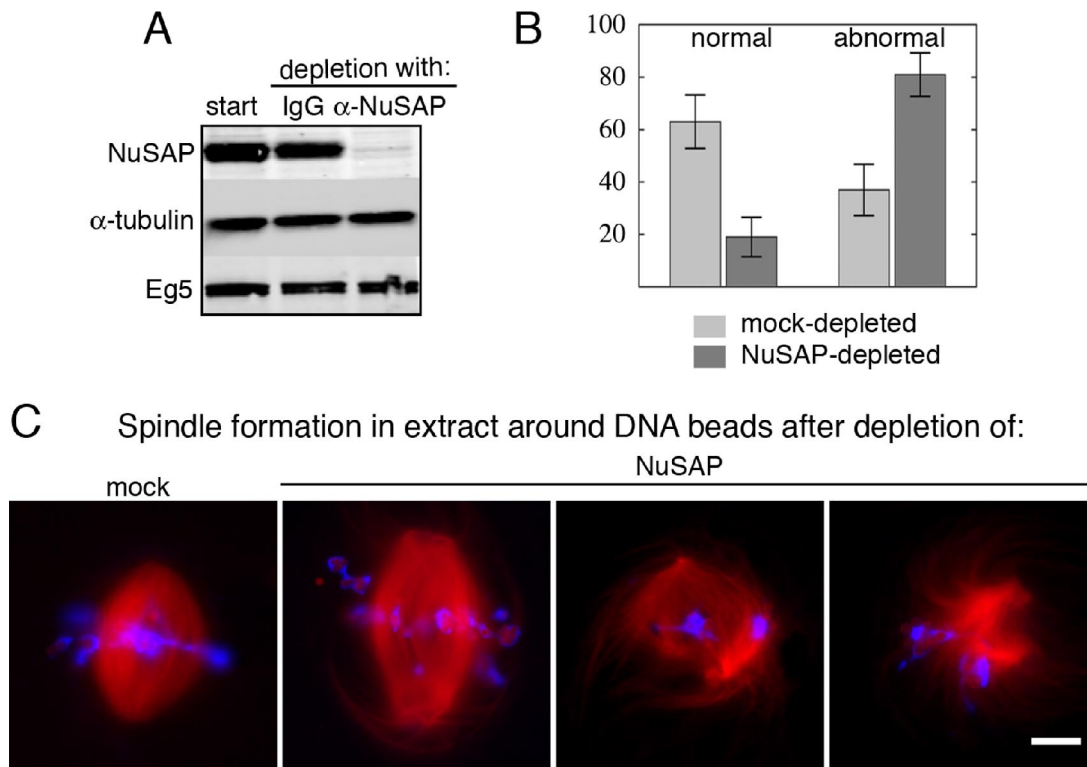### NuSAP Function Is Critical for Spindle Formation in Xenopus Egg Extract

To analyze the function of NuSAP in meiotic spindle formation, we prepared extracts from *Xenopus* eggs arrested in metaphase of meiosis II (CSF-arrested extracts). NuSAP was immunodepleted from the extracts by affinity-purified antibodies, and spindle assembly was allowed to proceed around DNA beads for 60 min at 20°C (Heald *et al.*, 1996; Desai *et al.*, 1999). DNA beads were used in this experiment instead of purified *Xenopus* sperm chromatin (Lohka and Masui, 1984) to ensure that NuSAP, which is a nuclear

protein, was not added to the depleted extracts with the sperm nuclei.

At depletion levels of ~90% (Figure 2A), microtubules were still produced around DNA beads (Figure 2C). However, we observed different defects in spindle organization. In some cases, microtubules formed distorted bipolar arrays that contained many buckled microtubules and had inconsistent pole-to-chromatin distances (Figure 2C, third panel). Moreover, although the spindle microtubules were usually still focused at the poles, they often appeared poorly organized around chromatin (Figure 2C, third panel). The microtubule density around chromatin often appeared to be reduced (Figure 2C, third panel). In extreme cases, spindles were impaired in establishing or maintaining bipolarity, and spindle poles were not located on opposite sides of the chromatin (Figure 2C, right panel). To quantify the defects we collectively categorized all spindles that were not of compact bipolar shape as abnormal and determined their percentage in four different experiments. The percentage of abnormal spindles was significantly increased in NuSAP-depleted extracts (more than 80% compared with 40% in mock-depleted extracts; Figure 2B). Thus, NuSAP appears to be essential for the proper assembly of meiotic spindles.

Two problems complicated the interpretation of this experiment. First, it was exceedingly difficult to deplete NuSAP to more than 90% from the extracts (Figure 2A). The residual NuSAP may be sufficient to provide partial function and lead to an underestimation of the effects of NuSAP depletion. Second, add-back of recombinant NuSAP to depleted extracts restored microtubule bundling but did not produce well-organized spindles. The chromatin-associated microtubules were strongly bundled (our unpublished data; but see Figure 3B), but other defects, such as impaired positioning of the spindle poles, were not rescued by recombinant NuSAP alone. Thus, either the recombinant protein was not fully functional or factors that codepleted with

Figure 2. NuSAP function is critical for spindle formation in *Xenopus* egg extract. (A) NuSAP protein was immunodepleted from meiotic *Xenopus* egg extract with an affinity-purified α-NuSAP antibody. Western blot analysis shows that this resulted in the reduction of NuSAP protein levels by ~90%, whereas the levels of α-tubulin and Eg5 protein were not detectably affected. (B and C) After NuSAP depletion, chromatin beads were prepared in NuSAP- or mock-depleted CSF extracts, and the beads were then placed in the depleted extracts to induce spindle assembly. After 60 min, the samples were fixed, and pictures were taken. Tubulin is shown in red, and the DNA beads are shown in blue. The left panel shows a control chromatin bead spindle formed in mock-depleted extract, the second panel from the left shows a normal spindle formed in NuSAP-depleted extract, and the two right panels show two examples of spindles that were categorized as abnormal. The percentage of abnormal spindles that formed in mock- and NuSAP-depleted extracts was determined in four independent experiments, each with 50 structures. Bars indicate mean values ± standard deviations. Bar, 10 μm.

NuSAP contribute to the production of the defects. We are currently addressing this problem. In summary, it appears that NuSAP activity is required to establish and/or maintain spindle integrity. The observed defects point toward a function of NuSAP in organizing chromosome-proximal microtubules. However, from these experiments we are unable to conclude whether this effect is direct or indirect.

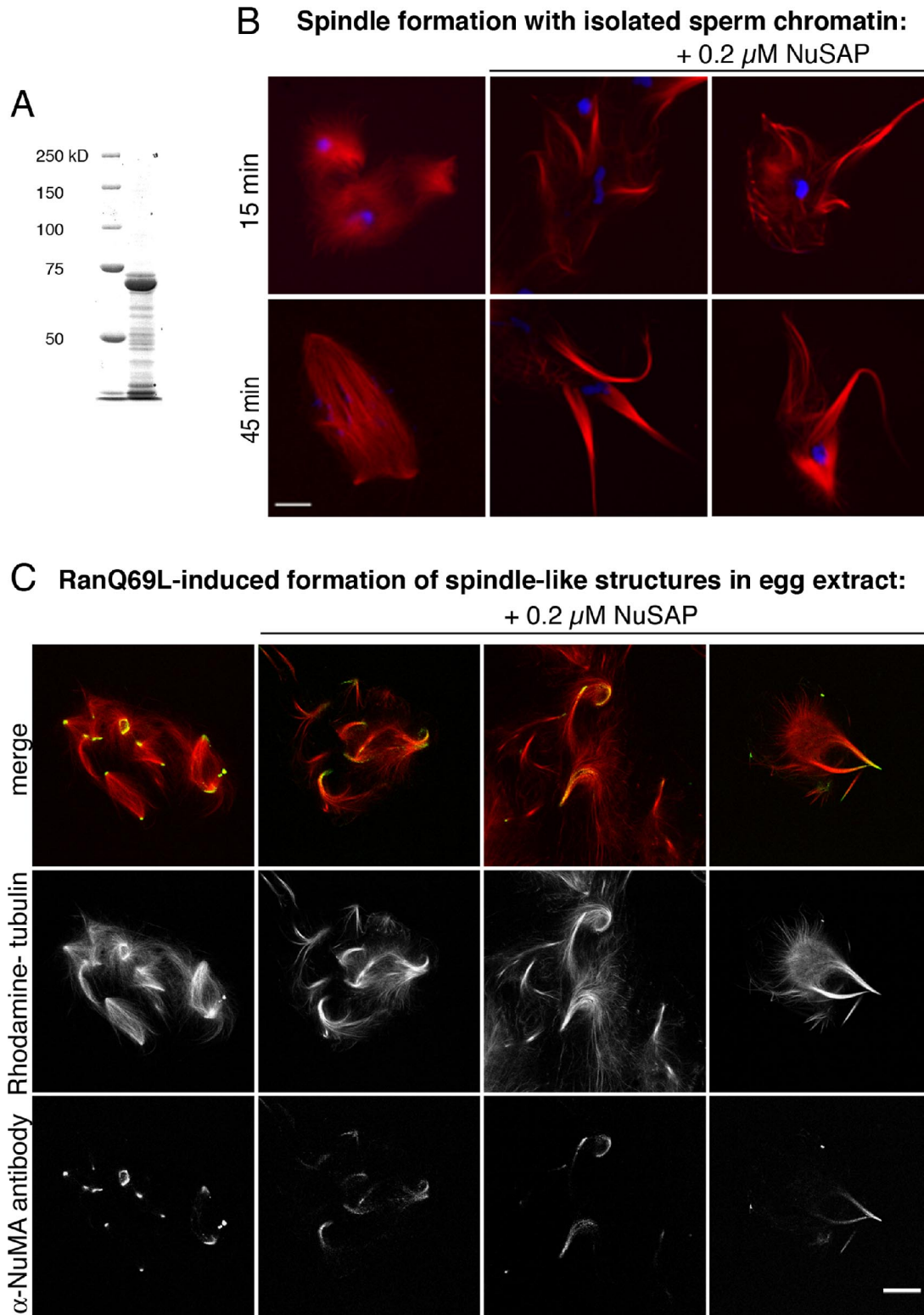### NuSAP Efficiently Bundles Spindle Microtubules in Meiotic Egg Extract

In the next step, we studied the effect of excess NuSAP on spindle assembly around sperm chromatin in *Xenopus* egg extracts (Figure 3B). When surplus NuSAP was added to the extract before the onset of spindle assembly, the spindle reactions were highly inefficient, and only a few chromatin samples acquired microtubules. It appeared that the presence of excess NuSAP blocked spindle formation. As an alternative approach, we therefore tested the effect of surplus NuSAP on already existing spindle structures. Isolated sperm chromatin was added to egg extract, and spindle assembly was allowed to proceed for either 15 or 45 min. Thereafter, the spindle reaction was supplemented with 0.2 μM recombinant NuSAP (4–10 times the endogenous NuSAP concentration) and further incubated for 10 min. The addition of surplus NuSAP had two reproducible effects on the majority (>90%) of the spindle structures (Figure 3B). First, the spindle microtubules became strongly bundled

into prominent fibers, and second, they often appeared to grow longer than the microtubules in control spindles.

The strength of the effect on spindle intermediates depended on the concentration of recombinant NuSAP added. At concentrations below 0.2 μM (0.05 and 0.1 μM were tested), the bundling of microtubules was still detectable, but less prominent, and fewer spindle structures were affected. In contrast, at concentrations above 0.5 μM, the spindles structures became strongly distorted and often lost their bipolar configuration.

The function of NuSAP was also probed in the context of chromatin-free spindle assembly mediated by RanQ69L. RanQ69L is a mutant of Ran that is locked in the active, GTP-bound state (Bischoff *et al.*, 1994). Like chromatin, RanQ69L activates a set of spindle assembly factors such that microtubule asters and bipolar spindle-like structures emerge (see *Introduction*).

When recombinant NuSAP alone was added to the egg extract, no detectable microtubule structures were formed (our unpublished data). This means that NuSAP activity is either inhibited or requires additional factors to efficiently produce microtubules in the extract. In contrast, the addition of 15 μM RanQ69L resulted in the formation of microtubules and their organization into asters, which over time evolved into bipolar spindle-like structures (Figure 3C). To analyze the effect of surplus NuSAP in chromatin-free spindle organization, the reaction was initiated with 15 μM RanQ69L.

B **Spindle formation with isolated sperm chromatin:**

A

Figure 3. NuSAP efficiently bundles spindle microtubules in egg extract. (A) Recombinant full length *Xenopus* NuSAP was expressed in *Escherichia coli* from pQE80 and purified via nickel-agarose and subsequent gel filtration. The marker (left lane) shows that recombinant NuSAP (right lane) runs at 70 kDa, slightly higher than its calculated molecular mass of 59 kDa. (B) Spindles were formed around sperm chromatin in CSF extract (Lohka and Masui, 1984; Desai *et al.*, 1999). For visualization of tubulin, the extract was spiked with rhodamine-labeled tubulin. After 15 or 45 min, 0.2 μM recombinant NuSAP was added to the extract. After 10 min of further incubation, the samples were fixed and analyzed by confocal microscopy. Tubulin is shown in red, and DNA is shown in blue. In the presence of surplus NuSAP, the spindle microtubules became strongly bundled and often appeared to grow longer than the microtubules in control samples. (C) RanQ69L (15 μM) was added to CSF extract to induce the assembly of chromatin-free spindle structures. After 30-min incubation at 20°C, bipolar

After 30 min, when Ran-spindles had reached the bipolar state, 0.2 μM recombinant NuSAP was added. The spindle reaction was allowed to proceed for a further 10 min before the samples were fixed (Figure 3C).

To monitor the position of spindle poles in chromatin-free spindles, a fluorescently labeled antibody of the spindle pole marker NuMA was added to the reaction (Merdes *et al.*, 1996; Mitchison *et al.*, 2005). The addition of surplus NuSAP to bipolar structures resulted in a strong bundling and extension of microtubules. Interestingly, the tips of the spindle poles were strongly curled. Moreover, NuMA became spread along the spindle axis instead of being tightly focused at the poles. Furthermore, the symmetric bipolar configuration of the spindles often appeared distorted. Together, these observations indicate that in the presence of surplus NuSAP, microtubules within spindle-like structures are excessively bundled, leading to aberrant spindle morphology.

NuSAP Converts Growing Microtubules into Aster-like Structures and Thick Fibers

Next, we probed the effect of recombinant NuSAP on purified tubulin. Recombinant NuSAP (1 μM) was added to different concentrations of soluble tubulin from 3 to 24 μM, and the reaction was incubated at 37°C for 15 min (Figure 4A). At 3 μM tubulin, NuSAP produced mainly small, aster-like structures with a dense tubulin core and short microtubules emanating from the center. At higher tubulin concentrations (6–24 μM; Figure 4A), NuSAP produced not only asters but also prominent microtubule fibers. The NuSAP-generated microtubule fibers became longer and more abundant with increasing tubulin concentrations (Figure 4A). In control samples, both the aster-like structures and the prominent microtubule fibers as were detectable with 6, 12, or 24 μM tubulin were absent. Thus, in the presence of NuSAP, net microtubule polymerization was significantly increased compared with the buffer control.

NuSAP is a highly basic protein with an isoelectric point of 9.9 and might cause nonspecific aggregation of tubulin. To test this possibility, we analyzed the effect of other highly basic proteins (a mixture of core histones) on pure tubulin (Supplemental Figure 1). While the NuSAP-generated structures contained microtubules and thus reflected some degree of organization, histones appeared to induce formation of disorganized aggregates of tubulin (Supplemental Figure 1). This indicates that the formation of NuSAP-asters is not due to nonspecific aggregation but the result of specific interaction.

The coexistence of two morphologically different structures is at first sight puzzling and may have two different explanations: First, the asters may represent early intermediates that evolve into microtubule fibers. Second, asters and fibers may result from two independent functions of NuSAP. We will return to this point later.

We used electron microscopy to obtain further insight into the organization of NuSAP and microtubules in the previously examined conditions. Thick bundles with closely adjacent microtubules were detected (Figure 4B). The intercon- nected microtubules displayed a strong tendency for parallel alignment. NuSAP itself formed irregularly shaped structures along the outside walls of the microtubules, without any detectable preference for the microtubule ends. NuSAP strongly accumulated on the microtubule bundles and was largely absent from microtubule-free regions, suggesting that its local concentration at the bundles is due to specific interaction with the microtubules. NuSAP alone gave rise to a small number of aggregates (Figure 4B). At the bundles, NuSAP appeared to fill the space between individual microtubules. Many microtubules were packed into bundles (Figure 4B), whereas others were cross-linked via their ends to form chains (Figure 4B, top left).

Importantly, the NuSAP–microtubule bundles not only contained intact microtubules but also prominent sheets consisting of long protofilaments (Figure 4B, top left, arrowheads; and enlargement, top right). Such prominent sheets were rarely detected in samples without NuSAP. This suggests that NuSAP efficiently promotes either the assembly or the maintenance of protofilament tubulin sheets.

These experiments revealed two properties of NuSAP. First, it appears to strongly promote the net production of microtubules and protofilaments. Second, it can efficiently cross-link microtubules into asters and thick fibers.

Recombinant NuSAP Can Efficiently Cross-Link Pure Microtubules and Tubulin Sheets and Stabilize Them against Depolymerization

NuSAP could in principle promote the production of microtubules and tubulin sheets by two different mechanisms. It may catalyze the assembly of tubulin dimers into protofilaments and microtubules. Alternatively, it may stabilize spontaneously formed microtubules and protofilaments against depolymerization.

We designed an assay to directly test whether NuSAP can stabilize microtubules, i.e., prevent the disassembly of dynamically unstable microtubules. Microtubules were first assembled at 50 μM, a concentration well above the critical tubulin concentration for polymerization (15 μM). Then, the microtubules were diluted to 5 μM, a concentration at which unstabilized microtubules rapidly disassemble. The dilution buffer contained GTP alone, or GTP plus recombinant NuSAP at different concentrations. In the absence of NuSAP, microtubules disassembled rapidly and none were detectable by fluorescent microscopy after 5 min (Figure 5A). In contrast, when NuSAP was present, large networks of microtubules were detectable.

The microtubules detected in the presence of NuSAP may be due to stabilization of the provided microtubules. Alternatively, they may have been newly generated by NuSAP. To distinguish between these two possibilities, we repeated the experiment under conditions where de novo microtubule assembly is highly inefficient. As before, tubulin was polymerized at 50 μM and subsequently diluted to 5 μM in the presence or absence of 0.7 μM NuSAP. This time, however, the dilution buffer lacked GTP, and the reaction was stopped after 30 s. In these conditions, NuSAP did not induce microtubule production with soluble tubulin (Figure 5B, bottom). Figure 5B shows that when NuSAP was absent, microtubules had already disassembled 30 s after dilution to 5 μM. In contrast, in the presence of NuSAP, large fields of microtubules were seen. This suggests that NuSAP exerts its function by stabilizing prepolymerized microtubules and not by de novo polymerization.

To investigate NuSAP-mediated microtubule stabilization in a more quantitative way, we performed microtubule pelleting assays. The amount of tubulin in the pellet reflects the

Figure 3 (cont). spindle-like structures had formed. Then, 0.2 μM recombinant NuSAP was added to the structures, and the reaction was incubated for a further 10 min. This treatment caused a tight bundling of the spindle microtubules, accompanied by a curling of the poles. Spindle poles were stained with an anti-NuMA antibody (shown in green). Bars, 10 μm (A and B).

A

tubulin (µM):

| 3 | 6 | 12 | 24 |

B

+ tubulin + NuSAP

NuSAP only   tubulin only
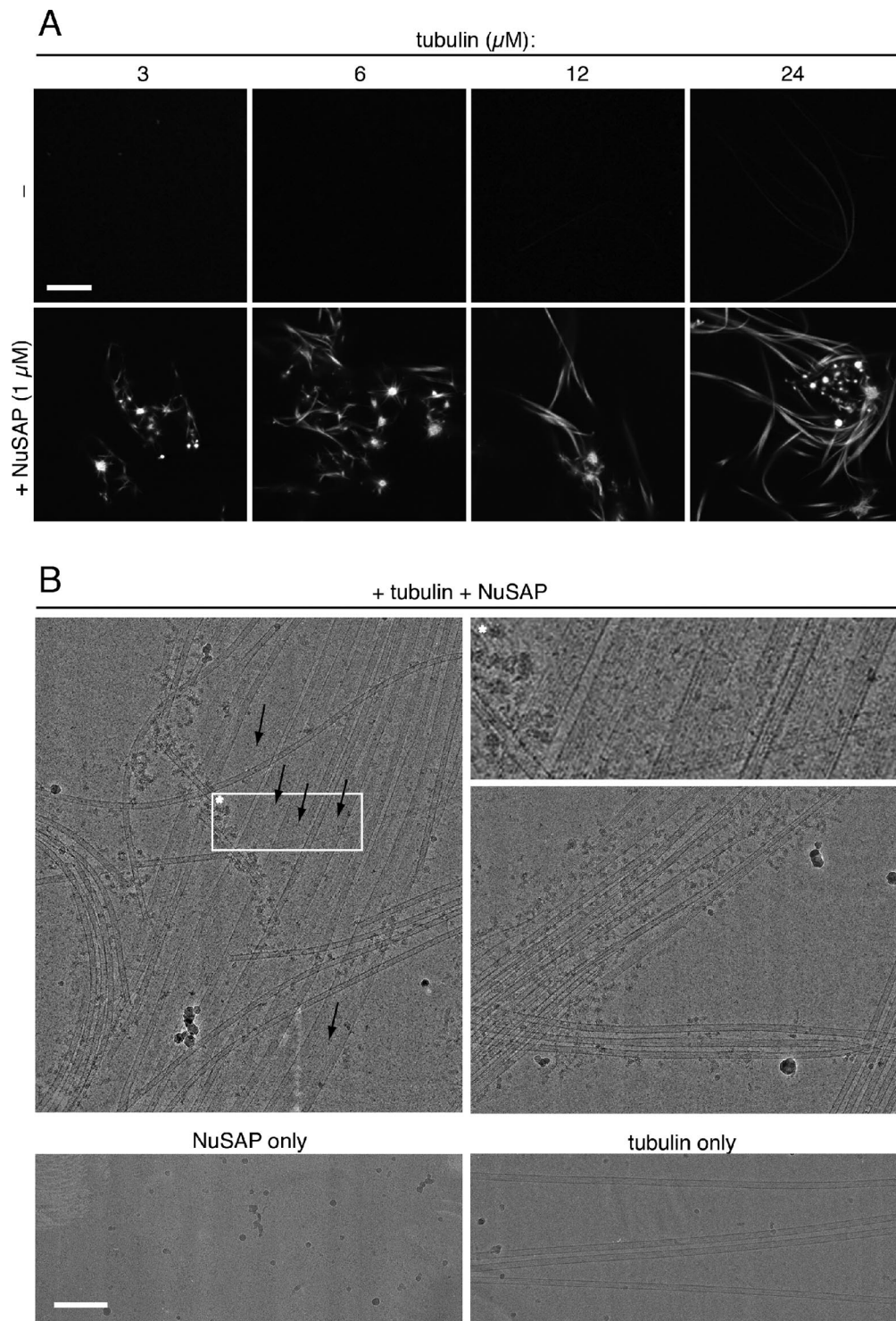
Figure 4. Recombinant NuSAP efficiently bundles and stabilizes pure microtubules. (A) Recombinant NuSAP (1 µM) was incubated with different concentrations of tubulin at 37°C for 10 min. The reaction was performed in BrB80 buffer with 1 mM GTP, and Ficoll and dextran as crowding reagents. At 3 and 6 µM tubulin, NuSAP produced mainly aster-like structures with short outgrowing microtubules. With increasing tubulin concentrations, NuSAP also gave rise to thick microtubule fibers. These fibers increased in length with increasing tubulin concentrations. (B) Purified tubulin (20 µM) was incubated in the presence or absence of 2 µM recombinant NuSAP in BrB80 buffer with 1 mM GTP at 37°C. After 10 min, the samples were fixed and prepared for cryoelectron microscopy (see *Materials and Methods*). In the presence of NuSAP, prominent bundles with closely adjacent microtubules were detectable. Note that not only intact microtubules but also protofilament sheets were in the bundles (arrowheads). NuSAP itself was detectable along the surface of, and between, microtubules. The top right panel shows a 2.8-fold enlargement of the protofilament sheets in the white box. Bars, 10 µm (A) and 100 nm (B).
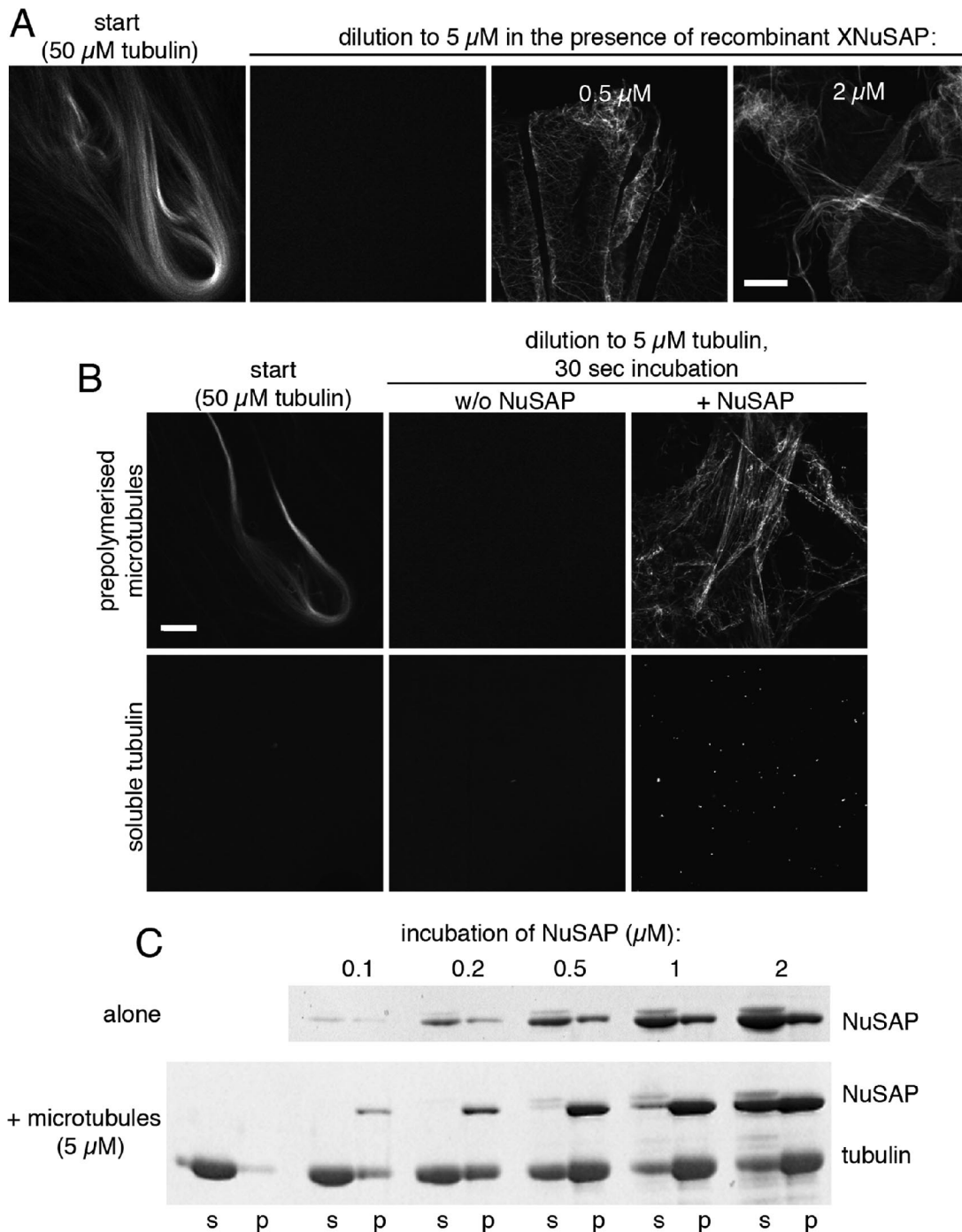
Figure 5. NuSAP can efficiently cross-link and stabilize pure microtubules. (A) Tubulin (50 μM) was polymerized in 20 mM HEPES-KOH, pH 7.5, 150 mM NaCl, and 1 mM GTP at 37°C for 10 min. Subsequently, microtubules were diluted to 5 μM tubulin concentration in the absence or presence of recombinant NuSAP at indicated concentrations. The reaction was incubated for 5 min at RT. (B) Microtubules were diluted from 50 to 5 μM tubulin into a buffer that lacked GTP, and, where indicated, contained 0.7 μM recombinant NuSAP. After 30-s incubation at RT, the samples were fixed and visualized by confocal microscopy. NuSAP efficiently stabilized preformed microtubules and organized them into networks. The lower panels show that NuSAP did not induce de novo microtubule production from soluble tubulin in these conditions. The microtubules in the networks often appeared fuzzy and irregular, indicating that NuSAP may not only cross-link and stabilize intact microtubules but also other polymerization intermediates. (C) Different concentrations of NuSAP were incubated either alone or with 5 μM microtubules. The reaction was incubated for 10 min at RT before soluble and polymerized tubulin were separated by ultracentrifugation. Pellet (p) and supernatant (s) were analyzed by SDS-PAGE and Coomassie staining. In the absence of NuSAP, most microtubules depolymerized. In contrast, with increasing concentrations of NuSAP, more and more microtubules were stabilized against depolymerization and tubulin thus occurred in the pellet. NuSAP alone precipitated to some extent. In contrast, in the presence of microtubules, NuSAP became absorbed to, and coprecipitated with, microtubules. Bars, 10 μm (A and B).
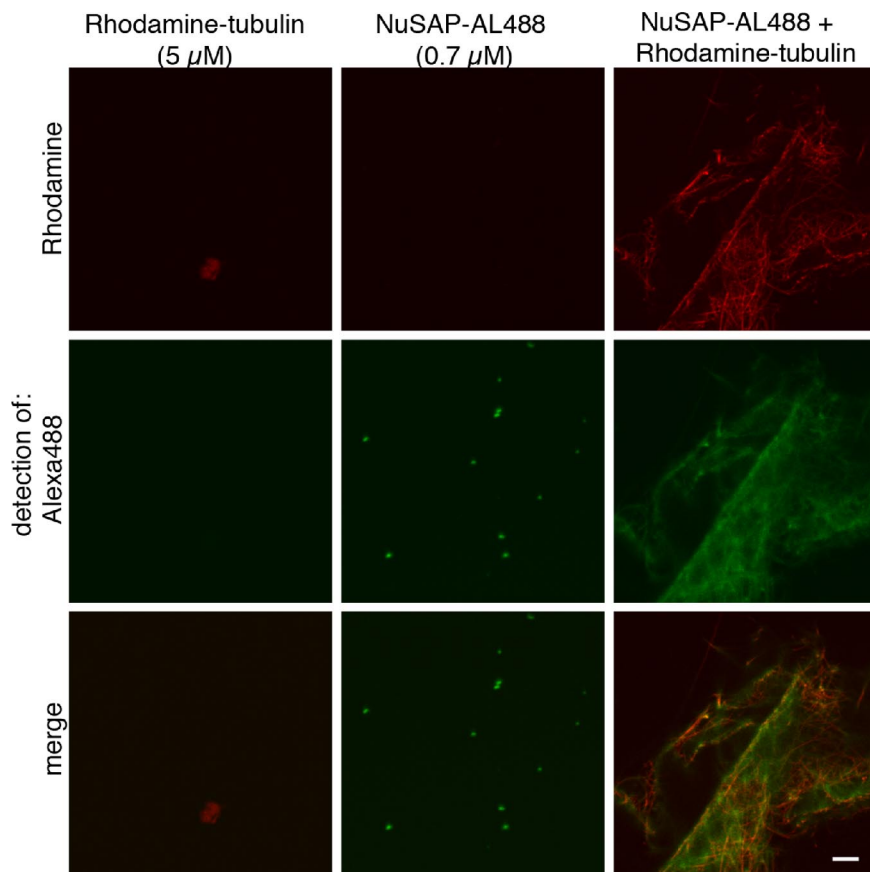
Figure 6. Alexa 488-labeled NuSAP accumulates at and near the surface of microtubules during stabilization. Rhodamine-tubulin (50 μM) was polymerized in 20 mM HEPES-KOH, pH 7.5, 150 mM NaCl, and 1 mM GTP at 37°C for 10 min and subsequently diluted to 5 μM tubulin concentration. In the absence of any further component (left), the microtubules disassembled rapidly, and none were detectable after 5 min. When Alexa 488-labeled NuSAP (0.7 μM) was present during dilution, the microtubules were stabilized and cross-linked (right). NuSAP localized along the surface of microtubules and also appeared to occupy the space between the cross-linked microtubules. In the absence of tubulin, NuSAP formed aggregates. Bar, 10 μm.

fraction of microtubules that are stabilized by NuSAP and thus remain in the polymerized, i.e., precipitable form. In agreement with the microscopy results in Figure 5, A and B, most of the microtubules depolymerized in the absence of NuSAP, whereas with increasing concentrations of NuSAP, more and more microtubules were stabilized against depolymerization (Figure 5C). NuSAP alone precipitated to some extent (Figure 5C, top). However, when microtubules were present, it efficiently coprecipitated with the microtubules (Figure 5C, bottom).

Remarkably, the microtubules that were stabilized by NuSAP did not remain individual, but instead were prominently cross-linked into large networks (Figure 5, A and B). This NuSAP-dependent microtubule cross-linking activity was exceedingly fast, being detectable after 30 s (Figure 5B). Importantly, other microtubule-interacting proteins such as TPX2 or EB1 did not produce such stabilized microtubule networks (our unpublished data), indicating that the capacity to both stabilize and cross-link microtubules is a specific property of NuSAP. Notably, not all tubulin structures in the networks had the compact and linear appearance of intact microtubules (Figures 5, A and B, and 6). Instead, numerous fuzzy structures and aggregates were detectable. This suggests that NuSAP stabilizes and cross-links not only intact microtubules but also other polymerization intermediates. Indeed, as depicted in Figure 4B, a significant proportion of NuSAP–microtubule bundles consisted of protofilament sheets.

The relative distribution of NuSAP and tubulin in the networks as detected by light microscopy is shown in Figure 6. NuSAP formed small, compact aggregates when incubated in the absence of microtubules (Figure 6, middle).

In contrast, in the presence of microtubules, NuSAP no longer formed aggregates but instead localized along, and maybe also between, the cross-linked microtubules (Figure 6).

Together, Figures 5 and 6 show that NuSAP is able to efficiently protect microtubules against depolymerization and that NuSAP can efficiently cross-link microtubules and possibly also other polymerization intermediates.

Impα, Impβ, and Imp7 Interact Directly with Recombinant NuSAP

A potent effector such as NuSAP is likely to be tightly regulated within the cell. It is a key finding of recent cell biology that certain mitotic factors are kept inactive by importin binding and that they are activated by RanGTP-dependent importin release (Hetzer *et al.*, 2002; Zheng, 2004). To determine whether potential regulators bind to NuSAP in a RanGTP-dependent manner, we immobilized NuSAP (zzNuSAP) and incubated it with meiotic *Xenopus* extract in the presence or absence of 20 μM RanQ69L. Two main binding partners bound to NuSAP that were released by RanQ69L (Figure 7A, lanes 2 and 3). Mass spectrometry identified them as Imp7 and Impβ. Subsequent Western blot analysis revealed Impα as one further interaction partner of NuSAP (our unpublished data; but see Figure 7B). Using recombinant factors, we verified that Impβ, Imp7, and the Impα/β heterodimer can interact with NuSAP directly (Figure 7B).

The interaction of Impα with NuSAP was independent of the presence of RanQ69L. This is expected, because Impα lacks a RanGTP binding site and is not a direct target of RanGTP. Notably, the RanQ69L-mediated dissociation of Impβ and Imp7 from NuSAP was not complete and indeed
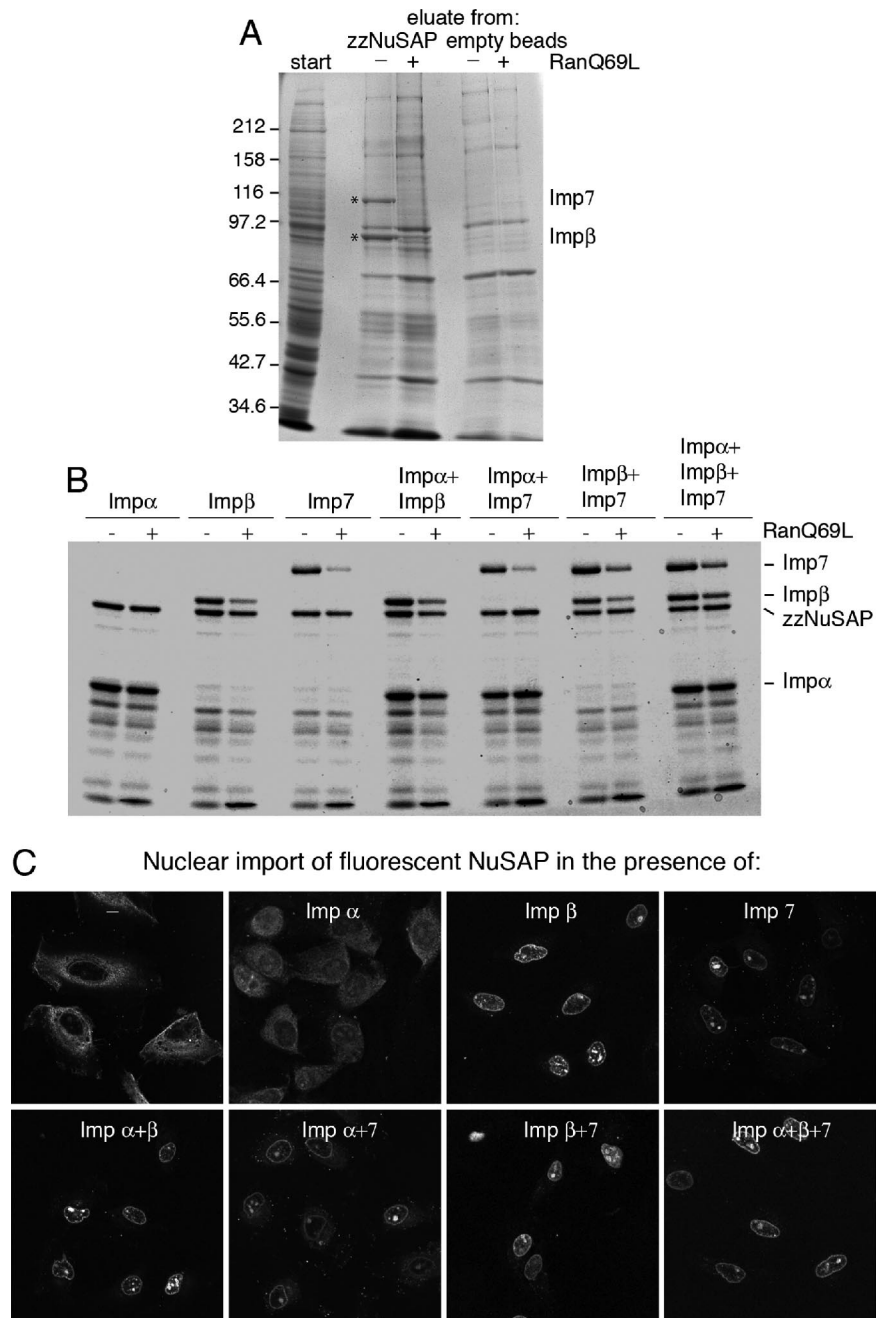
Figure 7. Recombinant NuSAP interacts directly with Impα, Impβ, and Imp7. (A) Immobilized zzNuSAP was incubated with CSF extract (start) in the presence or absence of 20 μM RanQ69L. The eluates from the zzNuSAP-matrix were analyzed by SDS-PAGE. Mass spectrometry identified Impβ and Imp7 as two proteins that interacted with NuSAP in a Ran-dependent manner. (B) Immobilized zzNuSAP was incubated with 2 μM recombinant Impα, Impβ, or Imp7 alone or in combinations. Where indicated, 35 μM RanQ69L was added. The eluates of the zzNuSAP column were analyzed by SDS-PAGE and Coomassie staining. The release of Impβ and Imp7 by RanQ69L was only partial. (C) The import of 0.7 μM fluorescent NuSAP into nuclei of permeabilized HeLa cells was studied. The import reaction contained an energy regenerating system, the core components of the RanGTPase system, and the indicated nuclear import receptors at 1.5 μM. The import reaction proceeded for 20 min at RT and was analyzed by live confocal microscopy. Impα and Impβ together, as well as Impβ and Imp7 alone, can mediate nuclear import of NuSAP. Bar, 10 μm.

rather inefficient when the importins were present simultaneously (Figure 7B). This may indicate that complexes consisting of NuSAP and the two importins cannot be dissociated by RanGTP alone.

To examine whether the NuSAP–importin interactions are functional, we analyzed whether the identified importins could mediate import of Alexa 488-labeled NuSAP into nuclei of permeabilized HeLa cells in a standard nuclear import assay (Figure 7C). In the absence of importins, NuSAP was largely excluded from the nuclei and remained cytoplasmic. This distribution did not significantly change when Impα was added. In contrast, in the presence of Impβ or Imp7 alone, NuSAP was efficiently removed from the cytoplasm and imported into the nuclei, where it accumulated at the nuclear rim and the nucleoli. Together, our data show

that Impα, Impβ, and Imp7 can directly interact with NuSAP. The Impα/β heterodimer, as well as Impβ and Imp7 alone, can mediate nuclear import of NuSAP.

Impα, -β, and -7 Impair the Ability of NuSAP to Form Microtubule Networks

Next, we probed whether the importins affect the ability of NuSAP to stabilize and cross-link microtubules into networks. As in Figure 5, tubulin was polymerized at 50 μM and subsequently diluted to trigger depolymerization. The dilution buffer contained 0.7 μM NuSAP alone or NuSAP and 5 μM of the individual importins. After 10-min incubation at RT, soluble and polymerized tubulin were separated by ultracentrifugation (Figure 8).
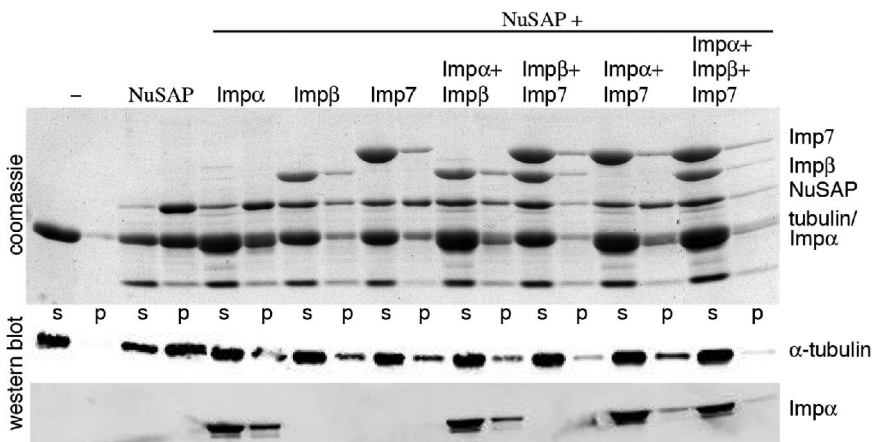
Figure 8. Impα, Impβ, and Imp7 impair the ability of NuSAP to form microtubule networks. Tubulin (50 μM) was polymerized in 20 mM HEPES-KOH, pH 7.5, 150 mM NaCl, and 1 mM GTP at 37°C for 10 min. Subsequently, the microtubules were diluted to 5 μM in a reaction buffer that contained 0.7 μM NuSAP and 5 μM importins in the indicated combinations. The samples were incubated at RT for 10 min and thereafter subjected to ultracentrifugation to separate soluble (s) from polymerized (p) tubulin. In the absence of NuSAP, the microtubules rapidly depolymerized and thus occurred in the soluble fraction. In contrast, NuSAP stabilized and cross-linked microtubules such that a large proportion of tubulin occurred in the pellet. Each importin reduced the ability of NuSAP to form microtubule networks, as the reduced amount of tubulin in the pellets indicates. The strongest inhibitory effect on NuSAP function was seen when all three receptors were present simultaneously.

The stabilizing and cross-linking activity of NuSAP, as determined by the amount of tubulin in the pellet, was decreased in the presence of either Impα, Impβ, or Imp7, indicating that each importin reduced the ability of NuSAP to form microtubule networks. Interestingly, Impβ not only suppressed the formation of the networks but also was able to rapidly dissolve preexisting NuSAP–microtubule networks (our unpublished data), suggesting that the microtubules within the NuSAP-induced networks are still potentially dynamic.

The inhibitory effect of the individual importins was not complete and did not increase when a threefold higher concentration of each importin was used (our unpublished data). Interestingly, the inhibition of microtubule stabilization was more efficient when Impβ and Imp7 were present simultaneously and nearly complete when all three receptors were provided (Figure 8). This suggests that the importins operate in an additive manner to block NuSAP function.

Impα, -β, and -7 Appear to Inhibit Different Aspects of NuSAP Function

Do the importins affect NuSAP function by the same mechanism? To address this question, we returned to the observation that NuSAP can convert soluble tubulin (at 6 μM and higher) into two morphologically distinct structures, asters and linear fibers (Figure 4). As mentioned, these two conformations possibly reflect two distinct activities of NuSAP. If so, this assay may be useful to probe the individual effects of the importins on NuSAP activity in more detail.

NuSAP (1 μM) was incubated with 15 μM soluble tubulin at 37°C for 15 min. Importins were present in the reactions at 5 μM and in combinations as indicated in Figure 9. As shown before, NuSAP alone efficiently converted 15 μM tubulin into asters and thick microtubule fibers. When Impα was present, neither long microtubule fibers nor small aster-like structures were detectable. Instead, small patches of tubulin were seen (Figure 9). In contrast, when Impβ was present, NuSAP almost exclusively produced long microtubule fibers, and only very few small asters emerged. Finally, on addition of Imp7, NuSAP apparently failed to generate long fibers and instead produced mainly small asters. These asters were on average smaller and consisted of fewer microtubules than the patches that emerged when Impα was present (Figure 9). The importins alone did not promote the production of microtubule structures (Supplemental Figure 2).

Thus, Impα, Impβ, and Imp7 appear to affect different aspects of NuSAP function. In the presence of Impα or Imp7, NuSAP was able to efficiently produce tubulin asters and patches, but it failed to promote the production of long microtubule fibers. In contrast, in the presence of Impβ, NuSAP efficiently produced long microtubules fibers; however, it apparently had lost its ability to generate asters. These results suggest that asters and linear microtubule fibers reflect two distinct functions of NuSAP.

Finally, we tested whether the inhibitory effect of the importins could be reversed by 15 μM RanQ69L (Figure 10). The addition of RanQ69L alone did not visibly affect the activity of NuSAP. The effect of Impα was not reversed by RanQ69L, indicating that the NuSAP–Impα interaction was not dissociated by RanQ69L. This is expected, because Impα does not directly interact with Ran. In contrast, the inhibitory effect of Impβ was efficiently reversed by RanQ69L, and NuSAP regained the ability to produce asters at an efficiency comparable with the control sample without importins. The inhibitory effect of Imp7 was only partially reversed by RanQ69L (Figure 10, fourth panel, top and bottom). This may suggest that the interaction between NuSAP and Imp7 is too strong to be efficiently released by RanQ69L alone.

DISCUSSION

We show here that *Xenopus* NuSAP localizes to meiotic spindles in *Xenopus* oocytes, where it appears enriched at spindle microtubules in the vicinity of chromatin. This chromatin-proximal localization at the spindle is so far unique among identified microtubule-interacting proteins. Valuable insight into NuSAP function came from its down-regulation in HeLa cells by RNA interference (Raemaekers *et al.*, 2003). Under knockdown conditions, spindles displayed morphological aberrations at all stages of mitosis. Microtubules appeared less compacted around chromatin, and chromosome capture, alignment, and segregation were inefficient. Moreover, during anaphase, the bulk of midzone microtubules was missing, and microtubules appeared depleted. As a complementary approach, we here studied the effect of NuSAP depletion from egg extracts on spindle assembly. Although spindle defects were observed after NuSAP depletion, the incompleteness of the NuSAP depletion and our failure to completely rescue the depletion phenotype made interpretation of these experiments difficult. However, we
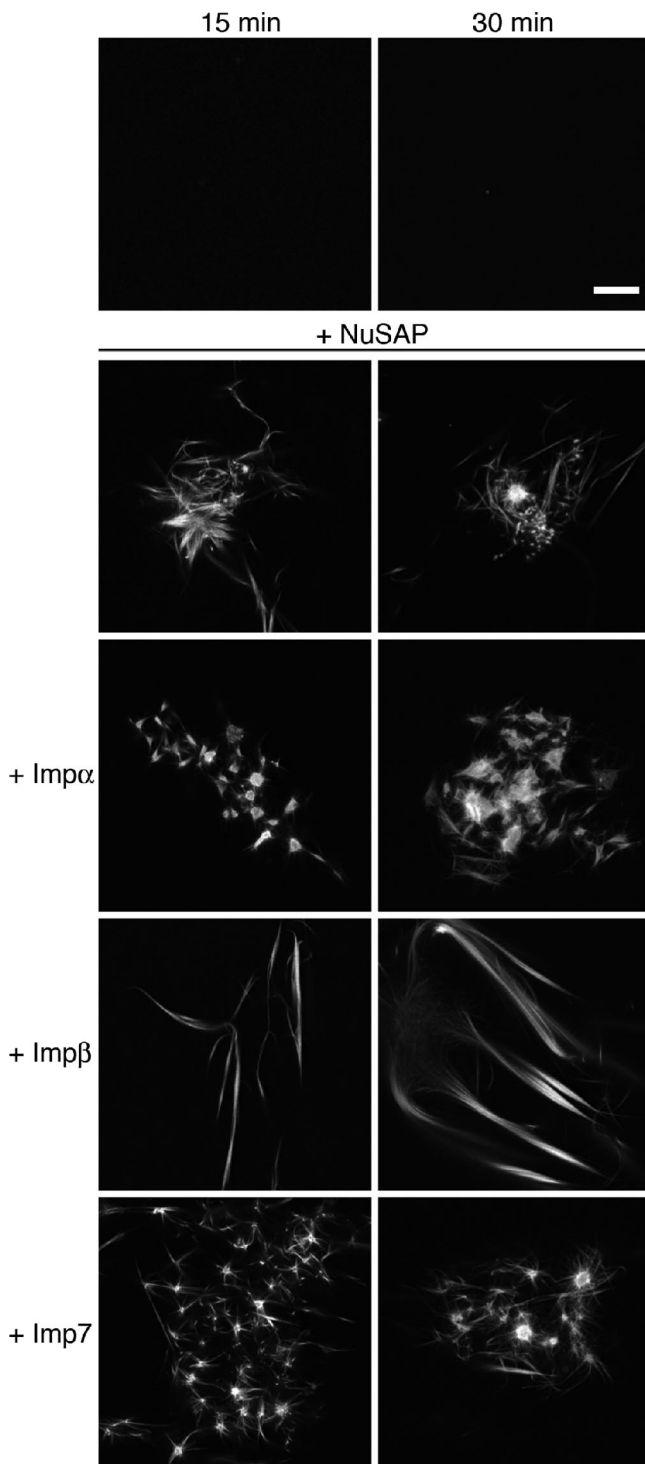
Figure 9. Impα, Impβ, and Imp7 appear to inhibit different aspects of NuSAP function. Tubulin (15 μM) was incubated in BrB80 buffer with 1 mM GTP, and Ficoll and dextran as crowding reagents. The top panels show 15- and 30-min incubations of the reaction in the absence of additional components. NuSAP (1 μM) was added to all other reactions either alone or with 5 μM importins as indicated. NuSAP produced two distinguishable structures, small asters with short microtubules, and long microtubule fibers. Each importin had a characteristic effect on NuSAP activity. In the presence of Impα, NuSAP formed compact aster-like structures and tubulin patches, but no long fibers. In the presence of Impβ, NuSAP generated long microtubule fibers, whereas small asters were missing. In the

can conclude that NuSAP, directly or indirectly, acts to establish and/or maintain spindle integrity. The observation that surplus NuSAP increases microtubule bundling in extract and the length of in vitro-assembled spindle-like structures points toward a microtubule-bundling and -stabilizing function of NuSAP at the spindle.

A more fruitful approach was to dissect NuSAP function in vitro with defined components. Experiments with low concentrations of preassembled microtubules revealed two immediate effects of NuSAP on tubulin. NuSAP efficiently stabilized microtubules against depolymerizing, and cross-linked microtubules into networks, asters, and bundles. Electron microscopy images provided interesting clues as to how NuSAP might interact with microtubules to achieve stabilization and cross-linking. First, the NuSAP–tubulin interactions gave rise not only to intact microtubules but also often to other intermediates that resembled sheets of tubulin filaments. Thus, NuSAP possibly not only stabilizes and cross-links intact microtubules but also other tubulin polymerization intermediates. Second, NuSAP appears to bind laterally to microtubule walls, without detectable preference for the microtubule ends, and furthermore appears to accumulate between neighboring microtubules. Hence, NuSAP possibly does not stabilize microtubules only by binding to the microtubule ends. Moreover, the EM data suggest that NuSAP may cross-link microtubules by crowding between adjacent microtubules. Further studies are required to elucidate more precisely how these morphological features relate to NuSAP's stabilizing and cross-linking functions.

Intriguingly, at tubulin concentrations above 6 μM, NuSAP produced both small asters and long microtubule fibers. Our data suggest that asters and fibers result from two separable activities of NuSAP. We assume that the stabilizing and cross-linking activities of NuSAP may operate independently and thus, at high tubulin concentrations, induce the formation of morphologically different structures. The stabilization activity promotes net polymerization of tubulin, which could explain the production of long prominent fibers. In contrast, cross-linking of microtubules in the absence of stabilization could lead to aster-like structures with short microtubules (Figure 9).

Several mitotic factors are regulated by the RanGTPase system via importins. During interphase, RanGTP dissociates importins from their import substrates inside the nucleus, whereas during mitosis, RanGTP releases importins from inhibitory interactions with their substrate molecules (Görlich, 1998; Hetzer et al., 2002; Groen et al., 2004; Zheng, 2004; Blower et al., 2005). NuSAP is a microtubule-binding protein that is actively imported into the nucleus during interphase (Raemaekers et al., 2003). This suggested that NuSAP may be subject to regulation by the Ran system. Indeed, our data show that NuSAP interacts directly with Impα, Impβ, and Imp7. Impβ is the prototype member of the Impβ protein superfamily. It can interact with its substrates in three different modes. In the simplest case, it can bind to its substrate directly. Examples of direct Impβ substrates are the HIV-1 Rev- and Tat-proteins (Henderson and Percipalle, 1997; Truant and Cullen, 1999); the ribosomal proteins L23a, S7, and L5 (Jäkel and Görlich, 1998); and the mRNA export protein Rae1, which is also involved in spindle organization (Blower et al., 2005). Second, Impβ can bind to its substrates indirectly via the import adapter Impα. The

presence of Imp7, NuSAP produced mainly small asters. The asters looked smaller than the patches that formed with NuSAP and Impα. Bar, 10 μm.

Configuration of pure tubulin in the presence of GTP, NuSAP and:
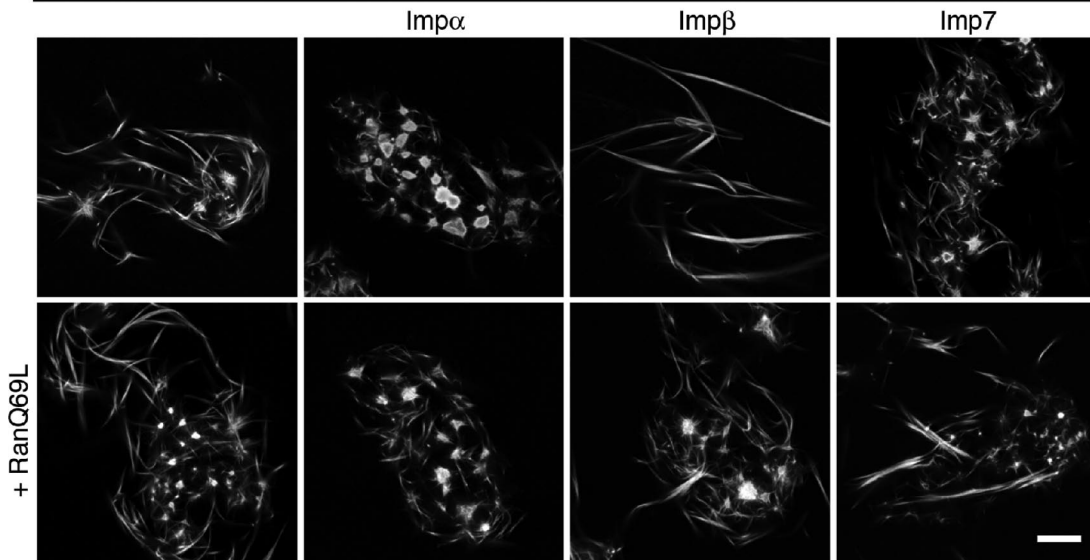
Figure 10. In the presence of microtubules, RanQ69L can efficiently reverse the effect of Impβ but not of Imp7. Tubulin (15 μM) was incubated in BrB80 buffer with 1 mM GTP, Ficoll and dextran as crowding reagents, and the indicated combinations of 1 μM NuSAP, 5 μM importins, and 15 μM RanQ69L. The reaction was incubated at 37°C for 10 min and subsequently analyzed by confocal microscopy. The addition of 15 μM RanQ69L had no effect on Impα, but it reversed the inhibitory effect of Impβ. For Imp7, the effect of RanQ69L was a partial reversal. Bar, 10 μm.

majority of identified nuclear import substrates are transported via this pathway. They interact with the Impα/β heterodimer via the classical monopartite or bipartite nuclear localization signals (Dingwall and Laskey, 1991; Görlich and Kutay, 1999). Third, Impβ has been shown to function in a heterodimer with Imp7 that mediates nuclear import of linker histones (Jakel *et al.*, 1999). Imp7 also operates as an autonomous import receptor for ribosomal proteins and possibly also other substrates (Jäkel and Görlich, 1998).

Our solution binding assay demonstrates that both Impβ and Imp7 bind to NuSAP directly and in apparently stoichiometric amounts. This, and the observation that both importins can individually mediate NuSAP import, may indicate that they function as autonomous receptors for NuSAP. Our data suggest that the Impα/β heterodimer can also bind to NuSAP and mediate its nuclear import.

All three transport receptors may therefore serve to bring about the nuclear localization of NuSAP in the intact interphase cell, thereby separating it from cytoplasmic microtubules. Importantly, our data indicate that the importins are direct negative regulators of NuSAP function at microtubules. Each importin appears to regulate a separate function of NuSAP. In the presence of Impβ, NuSAP generated long microtubule fibers but only few asters. This might suggest that in complex with Impβ, NuSAP can stabilize microtubules but not cross-link them efficiently into aster-like struc-
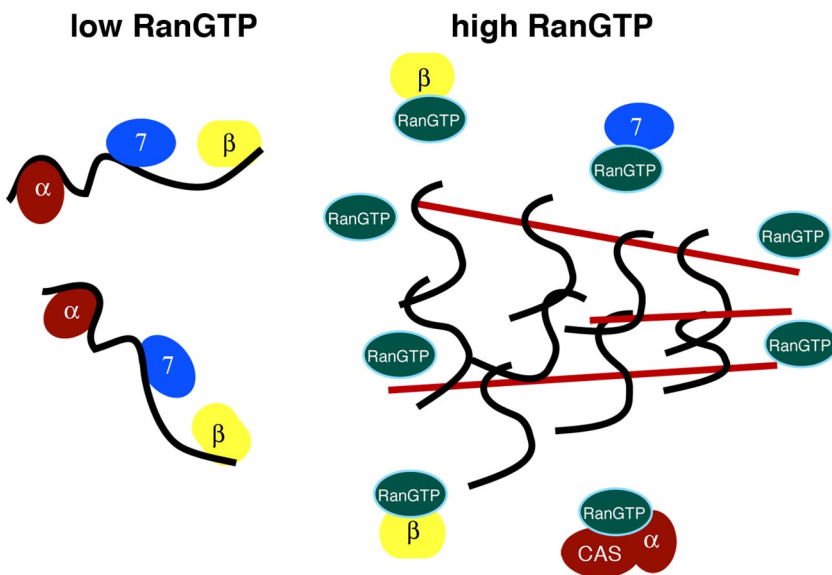
Figure 11. Model of NuSAP regulation by Impα, Impβ, and Imp7. At low RanGTP levels, Impα, Impβ, and Imp7 (colored circles) can bind simultaneously to NuSAP (black line) and thereby block its activity. At chromatin or inside the nucleus, high RanGTP levels cause the dissociation of all three receptors, resulting in full activation of NuSAP. Two immediate effects of NuSAP on tubulin have been revealed in this study: first, it can efficiently stabilize microtubules from depolymerizing, and second, it can cross-link microtubules into networks or fibers. We propose that, at the spindle, NuSAP acts to collect and stabilize spindle microtubules around chromatin and thereby aids to maintain spindle integrity.

tures. Imp7 showed the complementary result; only asters with very short microtubules formed, whereas long microtubule fibers were missing. Here, NuSAP appeared to fail to efficiently stabilize the microtubules, whereas its cross-linking activity was not detectably impaired. The effect of Impα appeared similar to that of Imp7 in the sense that long filaments rarely formed. Thus, Impα also appeared to reduce the stabilizing activity of NuSAP. The cross-linked products formed in the presence of Impα were, however, morphologically distinct from those seen in the presence of NuSAP alone or with Imp7. The observation that the individual importins are able to suppress distinct and specific aspects of NuSAP function suggests that the NuSAP protein domains that mediate cross-linking and stabilizing activity are likely to be distinct and that the individual importins interact with different parts of NuSAP.

Our results suggest that for NuSAP to be fully active, it must be dissociated from all three receptors. Both Impβ and Imp7 possess a RanGTP binding site and could be dissociated to some extent from NuSAP in vitro by RanQ69L. Their release in the solution binding assay was however not quantitative. This indicates that the presence of RanGTP alone does not suffice to dissociate NuSAP from Impβ and Imp7 and that NuSAP substrates such as microtubules may be necessary to achieve complete dissociation, analogous, for example, to the way that RNA is required to dissociate the yeast RNA binding protein Npl3p from its import receptor together with RanGTP (Senger et al., 1998).

Together, our data suggest the following model of NuSAP action (Figure 11). In the cell, RanGTP is generated at chromatin by its nucleotide exchange factor RCC1. During interphase, Impα, Impβ, and Imp7 together mediate import of NuSAP into the nucleus, where it is kept away from cytoplasmic microtubules. During mitosis, at distance from chromatin, all three importins can directly and simultaneously interact with NuSAP and thereby shield it from undesired or premature interactions with microtubules. At chromatin, RanGTP is present at high concentrations and here triggers the release of the importins from NuSAP, permitting its productive interactions with microtubules. As spindle microtubules are produced, NuSAP can rapidly cross-link and stabilize them around chromatin. How exactly NuSAP operates to cross-link microtubules is currently unclear. To actively cross-link two or more microtubules, NuSAP must either possess more than one microtubule binding site or have the ability to multimerize and thereby cross-link between microtubules. Local stabilization of microtubules at chromatin by NuSAP provides a high concentration of binding sites for motor proteins, which thereby become concentrated on the chromatin-proximal microtubules, where they can efficiently function to organize microtubules into a bipolar array.

What is the function of NuSAP at the spindle? Vertebrate spindles contain thousands of microtubules, many of which are not directly linked to chromatin or spindle poles. Diffusible motor proteins such as Eg5 can bundle microtubules (Sawin et al., 1992; Blangy et al., 1995; Gaglio et al., 1997; Walczak et al., 1998; Mayer et al., 1999; Kapitein et al., 2005). It is, however, conceivable that in the large vertebrate spindle, a second mechanism is needed to help the motors maintain spindle integrity. NuSAP, with its ability to cross-link and stabilize microtubules, would have the capacity to trap a large number of microtubules around chromosomes. NuSAP is present at the right position to fulfill this crucial function, namely, the central part of the spindle. This key function of NuSAP in holding microtubules together around chromatin would provide an explanation for the phenotype

that arises both after depletion of NuSAP by RNAi in HeLa cells (Raemaekers et al., 2003) and when present in surplus in *Xenopus* egg extract (Figure 3). In the depletion condition, spindles tend to disintegrate and microtubules around chromatin drift apart, leading to impaired chromosome alignment during metaphase, whereas when added in excess, NuSAP has the contrary effect and excessively bundles and stabilizes microtubules.

REFERENCES

Adam, S. A., Marr, R. S., and Gerace, L. (1990). Nuclear protein import in permeabilized mammalian cells requires soluble cytoplasmic factors. J. Cell Biol. *111*, 807–816.

Bischoff, F. R., Klebe, C., Kretschmer, J., Wittinghofer, A., and Ponstingl, H. (1994). RanGAP1 induces GTPase activity of nuclear Ras-related Ran. Proc. Natl. Acad. Sci. USA *91*, 2587–2591.

Blangy, A., Lane, H. A., d'Herin, P., Harper, M., Kress, M., and Nigg, E. A. (1995). Phosphorylation by p34cdc2 regulates spindle association of human Eg5, a kinesin-related motor essential for bipolar spindle formation in vivo. Cell *83*, 1159–1169.

Blower, M. D., Nachury, M., Heald, R., and Weis, K. (2005). A Rae1-containing ribonucleoprotein complex is required for mitotic spindle assembly. Cell *121*, 223–234.

Brinkley, B. R. (1985). Microtubule organizing centers. Annu. Rev. Cell Biol. *1*, 145–172.

Carazo-Salas, R. E., Guarguaglini, G., Gruss, O. J., Segref, A., Karsenti, E., and Mattaj, I. W. (1999). Generation of GTP-bound Ran by RCC1 is required for chromatin-induced mitotic spindle formation. Nature *400*, 178–181.

Chi, N. C., Adam, E.J.H., and Adam, S. A. (1997). Different binding domains for Ran-GTP and Ran-GDP/RanBP1 on nuclear import factor p97. J. Biol. Chem. *272*, 6818–6822.

Desai, A., Murray, A., Mitchison, T. J., and Walczak, C. E. (1999). The use of *Xenopus* egg extracts to study mitotic spindle assembly and function in vitro. Methods Cell Biol. *61*, 385–412.

Dingwall, C., and Laskey, R. A. (1991). Nuclear targeting sequences-a consensus? Trends Biochem. Sci. *16*, 478–481.

Dubochet, J., Adrian, M., Chang, J. J., Homo, J. C., Lepault, J., McDowall, A. W., and Schultz, P. (1988). Cryo-electron microscopy of vitrified specimens. Q. Rev. Biophys. *21*, 129–228.

Fornerod, M., Ohno, M., Yoshida, M., and Mattaj, I. W. (1997). Crm1 is an export receptor for leucine rich nuclear export signals. Cell *90*, 1051–1060.

Gaglio, T., Dionne, M. A., and Compton, D. A. (1997). Mitotic spindle poles are organized by structural and motor proteins in addition to centrosomes. J. Cell Biol. *138*, 1055–1066.

Görlich, D. (1998). Transport into and out of the cell nucleus. EMBO J. *17*, 2721–2727.

Görlich, D., Dabrowski, M., Bischoff, F. R., Kutay, U., Bork, P., Hartmann, E., Prehn, S., and Izaurralde, E. (1997). A novel class of RanGTP binding proteins. J. Cell Biol. *138*, 65–80.

Görlich, D., and Kutay, U. (1999). Transport between the cell nucleus and the cytoplasm. Annu. Rev. Cell Dev. Biol. *15*, 607–660.

Görlich, D., Pante, N., Kutay, U., Aebi, U., and Bischoff, F. R. (1996). Identification of different roles for RanGDP and RanGTP in nuclear protein import. EMBO J. *15*, 5584–5594.

Groen, A. C., Cameron, L. A., Coughlin, M., Miyamoto, D. T., Mitchison, T. J., and Ohi, R. (2004). XRHAMM functions in ran-dependent microtubule nucleation and pole formation during anastral spindle assembly. Curr. Biol. *14*, 1801–1811.

Heald, R., Tournebize, R., Blank, T., Sandaltzopoulos, R., Becker, P., Hyman, A., and Karsenti, E. (1996). Self-organization of microtubules into bipolar spindles around artificial chromosomes in *Xenopus* egg extracts. Nature *382*, 420–425.

Henderson, B. R., and Percipalle, P. (1997). Interactions between HIV Rev and nuclear import and export factors: the Rev nuclear localisation signal mediates specific binding to human importin-beta. J. Mol. Biol. *274*, 693–707.

Hetzer, M., Bilbao-Cortes, D., Walther, T. C., Gruss, O. J., and Mattaj, I. W. (2000). GTP hydrolysis by Ran is required for nuclear envelope assembly. Mol. Cell *5*, 1013–1024.

Hetzer, M., Gruss, O. J., and Mattaj, I. W. (2002). The Ran GTPase as a marker of chromosome position in spindle formation and nuclear envelope assembly. Nat. Cell Biol. *4*, E177–E184.

Hyman, A., Drechsel, D., Kellogg, D., Salser, S., Sawin, K., Steffen, P., Wordeman, L., and Mitchison, T. (1991). Preparation of modified tubulins. Methods Enzymol. *196*, 478–485.

Izaurralde, E., Kutay, U., von Kobbe, C., Mattaj, I. W., and Gorlich, D. (1997). The asymmetric distribution of the constituents of the Ran system is essential for transport into and out of the nucleus. EMBO J. *16*, 6535–6547.

Jakel, S., Albig, W., Kutay, U., Bischoff, F. R., Schwamborn, K., Doenecke, D., and Gorlich, D. (1999). The importin beta/importin 7 heterodimer is a functional nuclear import receptor for histone H1. EMBO J. *18*, 2411–2423.

Jäkel, S., and Görlich, D. (1998). Importin beta, transportin, RanBP5 and RanBP7 mediate nuclear import of ribosomal proteins in mammalian cells. EMBO J. *17*, 4491–4502.

Kalab, P., Pu, R. T., and Dasso, M. (1999). The ran GTPase regulates mitotic spindle assembly. Curr. Biol. *9*, 481–484.

Kapitein, L. C., Peterman, E. J., Kwok, B. H., Kim, J. H., Kapoor, T. M., and Schmidt, C. F. (2005). The bipolar mitotic kinesin Eg5 moves on both microtubules that it crosslinks. Nature *435*, 114–118.

Karsenti, E., and Vernos, I. (2001). The mitotic spindle: a self-made machine. Science *294*, 543–547.

Kutay, U., Bischoff, F. R., Kostka, S., Kraft, R., and Görlich, D. (1997). Export of importin alpha from the nucleus is mediated by a specific nuclear transport factor. Cell *90*, 1061–1071.

Lohka, M. J., and Masui, Y. (1984). Roles of cytosol and cytoplasmic particles in nuclear envelope assembly and sperm pronuclear formation in cell-free preparations from amphibian eggs. J. Cell Biol. *98*, 1222–1230.

Mayer, T. U., Kapoor, T. M., Haggarty, S. J., King, R. W., Schreiber, S. L., and Mitchison, T. J. (1999). Small molecule inhibitor of mitotic spindle bipolarity identified in a phenotype-based screen. Science *286*, 971–974.

Merdes, A., Ramyar, K., Vechio, J. D., and Cleveland, D. W. (1996). A complex of NuMA and cytoplasmic dynein is essential for mitotic spindle assembly. Cell *87*, 447–458.

Mingot, J. M., Kostka, S., Kraft, R., Hartmann, E., and Gorlich, D. (2001). Importin 13, a novel mediator of nuclear import and export. EMBO J. *20*, 3685–3694.

Mitchison, T. J., Maddox, P., Gaetz, J., Groen, A., Shirasu, M., Desai, A., Salmon, E. D., and Kapoor, T. M. (2005). Roles of polymerization dynamics, opposed motors, and a tensile element in governing the length of *Xenopus* extract meiotic spindles. Mol. Biol. Cell *16*, 3064–3076.

Ohba, T., Nakamura, M., Nishitani, H., and Nishimoto, T. (1999). Self-organization of microtubule asters induced in *Xenopus* egg extracts by GTP-bound Ran. Science *284*, 1356–1358.

Ohtsubo, M., Okazaki, H., and Nishimoto, T. (1989). The RCC1 protein, a regulator for the onset of chromosome condensation locates in the nucleus and binds to DNA. J. Cell Biol. *109*, 1389–1397.

Raemaekers, T., Ribbeck, K., Beaudouin, J., Annaert, W., Van Camp, M., Stockmans, I., Smets, N., Bouillon, R., Ellenberg, J., and Carmeliet, G. (2003). NuSAP, a novel microtubule-associated protein involved in mitotic spindle organization. J. Cell Biol. *162*, 1017–1029.

Rexach, M., and Blobel, G. (1995). Protein import into nuclei: association and dissociation reactions involving transport substrate, transport factors, and nucleoporins. Cell *83*, 683–692.

Ribbeck, K., and Görlich, D. (2001). Kinetic analysis of translocation through nuclear pore complexes. EMBO J. *20*, 1320–1330.

Sawin, K. E., LeGuellec, K., Philippe, M., and Mitchison, T. J. (1992). Mitotic spindle organization by a plus-end-directed microtubule motor. Nature *359*, 540–543.

Schwab, M. S., Roberts, B. T., Gross, S. D., Tunquist, B. J., Taieb, F. E., Lewellyn, A. L., and Maller, J. L. (2001). Bub1 is activated by the protein kinase p90(Rsk) during *Xenopus* oocyte maturation. Curr. Biol. *11*, 141–150.

Senger, B., Simos, G., Bischoff, F. R., Podtelejnikov, A., Mann, M., and Hurt, E. (1998). Mtr10p functions as a nuclear import receptor for the mRNA-binding protein Npl3p. EMBO J. *17*, 2196–2207.

Shevchenko, A., Wilm, M., Vorm, O., and Mann, M. (1996). Mass spectrometric sequencing of proteins silver-stained polyacrylamide gels. Anal. Chem. *68*, 850–858.

Siomi, M. C., Eder, P. S., Kataoka, N., Wan, L., Liu, Q., and Dreyfuss, G. (1997). Transportin-mediated nuclear import of heterogeneous nuclear RNP proteins. J. Cell Biol. *138*, 1181–1192.

Truant, R., and Cullen, B. R. (1999). The arginine-rich domains present in human immunodeficiency virus type 1 tat and rev function as direct importin beta-dependent nuclear localization signals. Mol. Cell Biol. *19*, 1210–1217.

Walczak, C. E., Vernos, I., Mitchison, T. J., Karsenti, E., and Heald, R. (1998). A model for the proposed roles of different microtubule-based motor proteins in establishing spindle bipolarity. Curr. Biol. *8*, 903–913.

Wilde, A., and Zheng, Y. (1999). Stimulation of microtubule aster formation and spindle assembly by the small GTPase Ran. Science *284*, 1359–1362.

Zheng, Y. (2004). G protein control of microtubule assembly. Annu. Rev. Cell Dev. Biol. *20*, 867–894.